

The $\Delta(1232)$ at RHIC

Hendrik van Hees[†] and Ralf Rapp

Cyclotron Institute and Physics Department, Texas A&M University, College Station, Texas 77843-3366

E-mail: hees@comp.tamu.edu, rapp@comp.tamu.edu

Abstract. We investigate properties of the $\Delta(1232)$ and nucleon spectral functions at finite temperature and baryon density within a hadronic model. The medium modifications of the Δ consist of a renormalization of its pion-nucleon cloud and resonant $\pi\Delta$ scattering. Underlying coupling constants and form factors are determined by the elastic πN scattering phase shift in the isobar channel, as well as empirical partial decay widths of excited baryon resonances. For cold nuclear matter the model provides reasonable agreement with photoabsorption data on nuclei in the Δ -resonance region. In hot hadronic matter typical for late stages of central *Au-Au* collisions at RHIC we find the Δ -spectral function to be broadened by ~ 65 MeV together with a slight upward mass shift of 5-10 MeV, in qualitative agreement with preliminary data from the STAR collaboration.

PACS numbers: 25.75.-q, 21.65.+f, 12.40.-y

1. Introduction

At low energies, the main features of Quantum Chromodynamics (QCD) are confinement and the spontaneous breaking of chiral symmetry. The former implies that we only observe hadrons (rather than quarks and gluons), while the latter is believed to govern the (low-lying) hadron-mass spectrum. Lattice-QCD calculations predict a phase transition from nuclear/hadronic matter to a deconfined, chirally symmetric state [1] at temperatures $T \simeq 150$ -200 MeV, dictating a major reshaping of the hadronic spectrum in terms of degenerate chiral partners. The observation of such medium modifications is therefore an important objective in relativistic heavy-ion collision experiments.

Large theoretical efforts have been devoted to evaluate in-medium properties of vector mesons which are accessible experimentally through dilepton invariant-mass spectra [2]. In most of these studies, baryon-driven effects are essential to account for the dilepton enhancement observed in *Pb-Au* collisions at the SPS below the free ρ mass [3, 4]. Thus, changes in the baryon properties themselves deserve further investigation. In addition, recent measurements of πN invariant-mass spectra in nuclear collisions [5, 6, 7] may open a more direct window on modifications of the $\Delta(1232)$.

[†] presenting author

To date, in-medium properties of the Δ have mostly been assessed in cold nuclear matter [8, 9, 10, 11, 12, 13], with few exceptions [14, 15]. In this article we will discuss properties of the nucleon and the $\Delta(1232)$ in a hot and dense medium [16], employing a finite-temperature field theory framework based on hadronic interactions. Both direct interactions of the Δ with thermal pions as well as modifications of its free πN self-energy (including vertex corrections) will be accounted for.

The article is organised as follows. In Sec. 2 we introduce the hadronic Lagrangian and outline how its parameters are determined using scattering and decay data in vacuum. In Sec. 3 we compute in-medium self-energies for nucleon and Δ . In Sec. 4 we first check our model against photoabsorption cross sections on the nucleon and nuclei, followed by a discussion of the spectral functions under conditions expected to occur in high-energy heavy-ion collisions. We close with a summary and outlook.

2. Hadronic Interaction Lagrangians in Vacuum

The basic element of our analysis are 3-point interaction vertices involving a pion and two baryons, $\pi B_1 B_2$. Baryon fields are treated using relativistic kinematics, $E_B^2(\mathbf{p}) = m_B^2 + \mathbf{p}^2$, but neglecting anti-particle contributions and restricting Rarita-Schwinger spinors to their non-relativistic spin-3/2 components. Pions are treated fully relativistically ($\omega_\pi^2(\mathbf{k}) = m_\pi^2 + \mathbf{k}^2$). The resulting interaction Lagrangians are thus of the usual nonrelativistic form involving (iso-) spin-1/2 Pauli matrices, 1/2 to 3/2 transition operators, as well as spin-3/2 matrices [9, 17, 18, 19, 20], see Ref. [16] for explicit expressions. To simulate finite-size effects we employed hadronic form factors with a uniform cutoff parameter $\Lambda_{\pi B_1 B_2} = 500$ MeV (except for πNN and $\pi N\Delta$ vertices).

The imaginary part of the vacuum self-energy for the $\Delta \rightarrow N\pi$ decay takes the form

$$\text{Im}\Sigma_{\Delta}^{(N\pi)}(M) = -\frac{f_{\pi N\Delta}^2}{12m_\pi^2\pi} \frac{m_N k_{\text{cm}}^3}{M} F^2(k_{\text{cm}}) \Theta(M - m_N - m_\pi) \quad (1)$$

with k_{cm} the center-of-mass decay momentum (an extra factor $m_N/E_N(k_{\text{cm}})$ has been introduced in Eq. (1) to restore Lorentz-invariance), and the real part is determined via a dispersion relation. With a bare mass of $m_{\Delta}^{(0)}=1302$ MeV, a form-factor cutoff $\Lambda_{\pi N\Delta}=290$ MeV and a coupling constant $f_{\pi N\Delta} = 3.2$ we obtain a satisfactory fit to the experimental δ_{33} -phase shift [21, 15, 22].

To account for resonant interactions of the Δ with pions we identified the relevant excited baryons via their decay branchings $B \rightarrow \pi\Delta$. The pertinent coupling constants have been determined assuming the lowest partial wave to be dominant (unless otherwise specified) [23], using pole masses and (total) widths of the resonances. The same procedure has been adopted for resonant πN interactions (which are used to evaluate finite-temperature effects on the nucleon). The resonances included are $N(1440)$, $N(1520)$, $N(1535)$, $\Delta(1600)$, $\Delta(1620)$ and $\Delta(1700)$. The total widths figuring into the resonance propagators have been obtained by scaling up the partial πN and $\pi\Delta$ channels, and vacuum renormalizations of the masses have been neglected.

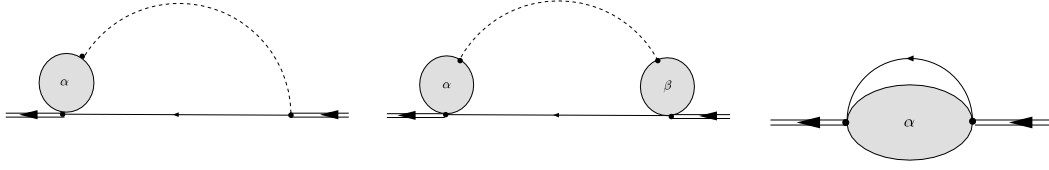


Figure 1. Diagrammatic representation of $\pi N \Delta$ vertex corrections (dashed lines: pion, solid lines: nucleon, double solid lines: $\Delta(1232)$); a bubble with label α corresponds to a Lindhard function Π_α ($\alpha \in \{1, 2\}$) attached to baryon lines with pertinent Migdal parameters, i.e., g'_{12} for $\alpha=1$ and g'_{22} for $\alpha=2$.

Finally, the evaluation of the photoabsorption cross section requires a $\gamma N \Delta$ vertex for which we employ the magnetic coupling [10]

$$\mathcal{L}_{\gamma N \Delta} = -\frac{f_{\gamma N \Delta}}{4\pi m_\pi} \psi_N^\dagger (\mathbf{S}^\dagger \times \nabla) \mathbf{A} T_3^\dagger \Psi_\Delta + \text{h.c.} \quad (2)$$

3. Self-energies at Finite Temperature and Density

The interactions described in the previous section are now used to evaluate the Δ self-energy in hot hadronic matter. The first modification concerns the πN loop which we obtain within the Matsubara formalism as

$$\begin{aligned} \Sigma_\Delta^{(N\pi)}(p) &= \frac{f_{\pi N \Delta}^2}{3m_\pi^2} \int \frac{d^4 l}{(2\pi)^4} \frac{m_N}{E_N(l)} \mathbf{k}^2 F_\pi^2(|\mathbf{k}|) \\ &\times \{ [\Theta(k_0) + \sigma(k_0) f^\pi(|k_0|)] A_\pi(k) G_N(l) - f^N(l_0) A_N(l) G_\pi(k) \}, \end{aligned} \quad (3)$$

where $k = p - l$ is the pion 4-momentum. The thermal distributions are defined by $f^N(l_0) = f^{\text{fermi}}(l_0 - \mu_N, T)$ and $f^\pi(|k_0|) = f^{\text{bose}}(|k_0|, T) \exp(\mu_\pi/T)$, with f^{fermi} and f^{bose} the Fermi and Bose functions, respectively. For simplicity, finite pion-chemical potentials, $\mu_\pi > 0$, are treated in the Boltzmann limit to avoid Bose singularities in the presence of broad pion spectral functions (a more detailed discussion of this point will be given elsewhere). In Eq. (3) positive energies $k_0 > 0$ correspond to outgoing pions, i.e., $\Delta \rightarrow \pi N$ decays, while $k_0 < 0$ accounts for scattering with (incoming) pions from the heat bath.

The key quantities in Eq. (3) are the in-medium pion and nucleon propagators, G_π and G_N , and pertinent spectral functions $A_N = -2\text{Im}G_N$ and $A_\pi = -2\text{Im}G_\pi$. The modifications of the pion propagator are implemented via a self-energy, arising from two parts: (i) interactions with thermal pions modeled by a four-point interaction in second order (“sunset diagram”) [24], with a coupling constant adjusted to qualitatively reproduce the results of more elaborate $\pi\pi$ interactions in s , p , and d -wave [25]; (ii) interactions with baryons via p -wave nucleon- and Δ -hole excitations at finite temperature, described by standard Lindhard functions, supplemented by short-range correlations encoded in Migdal parameters [26] (our default values are $g'_{NN}=0.8$, $g'_{N\Delta}=g'_{\Delta\Delta}=0.33$). These excitations induce a softening of the pion-dispersion relation which can even lead to a (near) vanishing of the pion group velocity at finite momentum, inducing an artificial threshold enhancement in the Δ self-energy [14]. This feature is

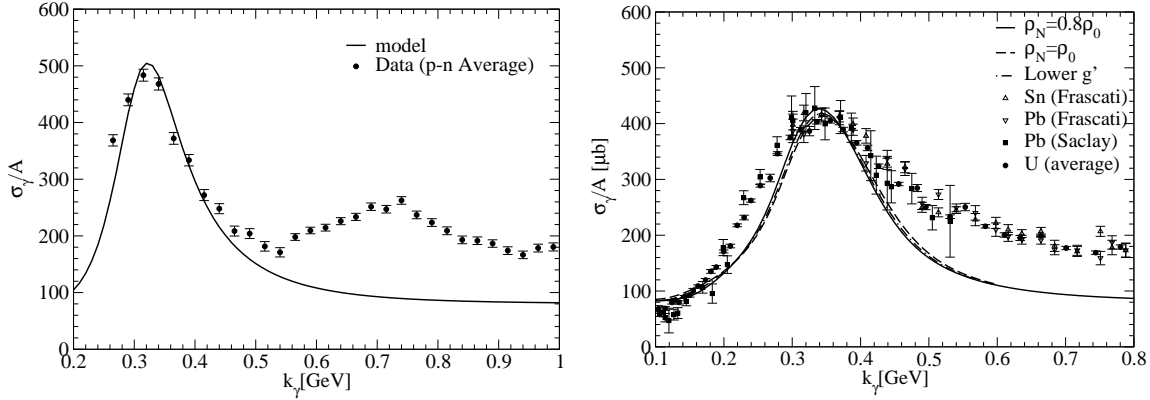


Figure 2. Photoabsorption cross sections on nucleons (left panel, data from [29]) and nuclei (right panel; data from [30, 31, 32, 33, 34, 35]).

remedied by accounting for appropriate vertex corrections, which in the case of $\rho \rightarrow \pi\pi$ decays are required to maintain a conserved vector current in the medium [27, 28]. Here we apply the same technique to the $\pi N\Delta$ vertex, cf. Fig. 1. The nucleon self-energy is calculated in terms of resonant interactions with thermal pions, at the same level of approximation as the pion Lindhard functions (i.e., neglecting off energy-shell dependencies in the spectral functions of the excited baryons).

The second contribution to the in-medium Δ self-energy consists of resonant $\pi\Delta \rightarrow B$ interactions, corresponding to the finite-temperature part of πB loops. The resulting self-energy expressions are similar to Eq. (3) but with only the scattering part ($k_0 < 0$) retained (note that this is consistent with our description of the $\Delta(1232)$ in vacuum where πB loops are not included).

4. In-medium Spectral Properties of the Δ

4.1. Photoabsorption on Nucleons and Nuclei

Valuable constraints on the Δ spectral function in cold nuclear matter can be obtained from photoabsorption cross sections on nuclei. To leading order in α_{em} , the latter can be related to the photon self-energy (electromagnetic current correlator), Π_γ , by [18]

$$\frac{\sigma_{\gamma A}^{\text{abs}}}{A} = \frac{4\pi\alpha}{k} \frac{1}{\varrho_N} \frac{1}{2} \text{Im}\Pi_\gamma(k_0 = k), \quad \Pi_\gamma = \frac{1}{2} g_{\mu\nu} \Pi^{\mu\nu}, \quad (4)$$

where $k_0 = k$ denotes the photon energy (momentum). With the vertex of Eq. (2) we evaluate the γ -induced Δ -hole loop using our full Δ propagator. The cross section for a nucleon target follows from the low-density limit ($\varrho_N \rightarrow 0$) of Eq. (4) involving the free Δ -spectral function, which we use to fix the coupling constant and form-factor cut-off of the $\gamma N\Delta$ vertex at $f_{\gamma N\Delta} = 0.653$ and $\Lambda_{\gamma N\Delta} = 400$ MeV, respectively, cf. left panel of Fig. 2 (we have also included an estimate of the nonresonant background of $80\mu\text{b}$ [18]). Taking an average nuclear density of $0.8\varrho_0$, our prediction for nuclei follows without further assumption, cf. right panel of Fig. 2. The sensitivity to changes in the

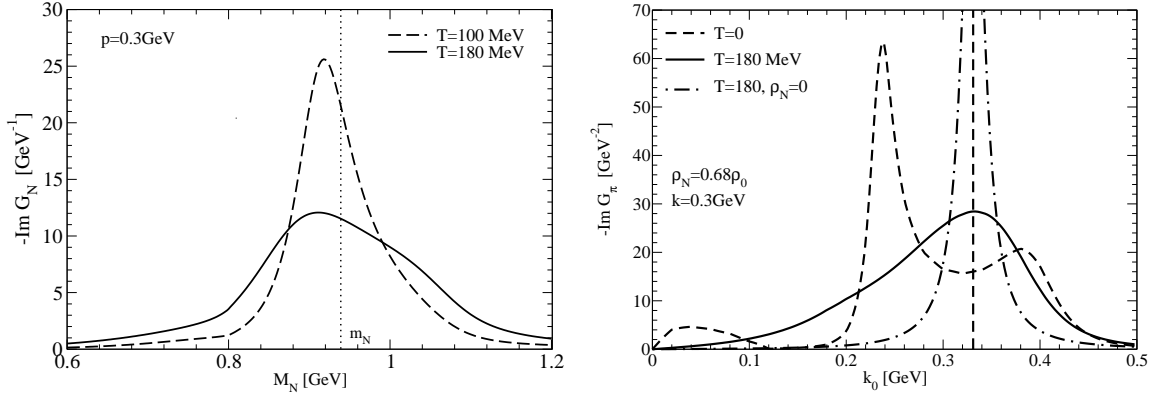


Figure 3. Left panel: nucleon spectral function at RHIC (solid line $T=180$ MeV, $\varrho_N=0.68\varrho_0$; dashed line: $T=100$ MeV, $\varrho_N=0.12\varrho_0$). Right panel: pion spectral function for cold nuclear matter (dashed line: $T=0$, $\varrho_N=0.68\varrho_0$) and at RHIC (solid line: $T=180$ MeV, $\varrho_N=0.68\varrho_0$); the dash-dotted line corresponds to switching off baryonic effects leaving only the 4-point interactions with thermal pions.

Migdal parameters or the nuclear density is very moderate. Given our rather simple approach for the cross section, the agreement with data is fair. The discrepancies at low energy (which seem to be present already for the nucleon) could be due to interference with the background, collective effects involving direct NN^{-1} -excitations, or transverse contributions with in-medium ρ mesons in the vertex corrections of the Δ decay. At higher energies, further resonances in the photon self-energy need to be included.

4.2. Hot Hadronic Matter

Let us finally turn to the results for hot hadronic matter. In heavy-ion collisions one expects a hierarchy of chemical freeze-out (determining the ratios of stable hadrons) and thermal freeze-out (where elastic rescattering ceases). The former is characterized by a temperature T_{chem} and a common baryon chemical potential μ_B . Thermal freezeout occurs at lower $T_{\text{fo}} \simeq 100$ MeV, which requires the build-up of additional chemical potentials for pions, kaons, etc. [36], to conserve the observed hadron ratios, including relative chemical equilibrium for elastic processes, e.g. $\pi N \leftrightarrow \Delta$ implying $\mu_\Delta = \mu_N + \mu_\pi$.

Under RHIC conditions the nucleon spectral function exhibits an appreciable broadening and a moderate downward mass shift (left panel of Fig. 3) due to resonant scattering off thermal pions. The pion spectral function (right panel of Fig. 3) is strongly broadened mostly due to scattering off baryons, with little mass shift. Thermal motion completely washes out the multi-level structure visible at zero temperature (dashed line). Also for the Δ spectral function (left panel in Fig. 4) the main effect is a broadening with a slight repulsive mass shift. Half of the increase of the in-medium width is due to baryon-resonance excitations (slightly enhanced due to in-medium pion propagators), adding to the contribution of the πN loop. In the real part, however, the predominantly repulsive contributions from baryon resonances are counterbalanced by net attraction in the πN loop (mostly due to the pion-Bose factor). At thermal freeze-out we find

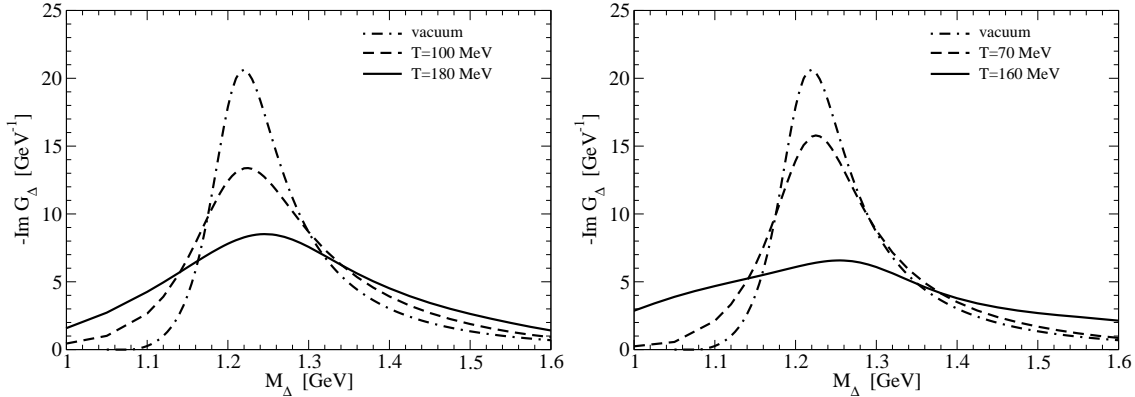


Figure 4. In-medium $\Delta(1232)$ spectral functions in heavy-ion collisions compared to free space (dash-dotted lines); left panel: RHIC; dashed line: $T=100$ MeV, $\varrho_N=0.12\varrho_0$ ($\mu_N=531$ MeV), $\mu_\pi=96$ MeV; solid line: $T=180$ MeV, $\varrho_N=0.68\varrho_0$ ($\mu_N=333$ MeV), $\mu_\pi=0$. Right: future GSI facility; dashed line: $T=70$ MeV, $\varrho_N=0.19\varrho_0$ ($\mu_N=727$ MeV), $\mu_\pi=105$ MeV; solid line: $T=160$ MeV, $\varrho_N=1.80\varrho_0$ ($\mu_N=593$ MeV), $\mu_\pi=0$.

a peak position at about $M \simeq 1.226$ GeV and a width $\Gamma \simeq 177$ MeV, to be compared to the corresponding vacuum values of $M \simeq 1.219$ GeV and $\Gamma \simeq 110$ MeV, in qualitative agreement with preliminary data from STAR [7]. For more conclusive comparison a detailed treatment of the freeze-out dynamics is mandatory. In the vicinity of T_c , the Δ width increases substantially. We expect this trend to be further magnified when including transverse parts in the vertex corrections, especially in combination with in-medium ρ -mesons [2].

In the right panel of Fig. 4 we show the Δ -spectral function in a net-baryon rich medium, representative for the future GSI facility. Whereas in dilute matter the line shape is only little affected, the resonance structure has essentially melted close to T_c , mostly due to a strong renormalization of the pion propagator at high density.

5. Conclusions and outlook

Based on hadronic interaction Lagrangians employed within a finite-temperature many-body approach we have evaluated medium effects on pions, nucleons and deltas. The resulting Δ -spectral functions in cold nuclear matter provide fair agreement with photoabsorption data on nuclei. In hot hadronic matter, we found a significant broadening and a slight upward peak shift of the Δ resonance, qualitatively in line with preliminary measurements of πN invariant-mass spectra at RHIC.

Future improvements of the $\pi N \Delta$ system in vacuum include u -channel exchange diagrams as well as spin-3/2- Δ^* excitations which we expect to increase the rather low form-factor cut-off used so far.

We further plan to implement in-medium baryon propagators into the description of axial-/vector mesons within a chiral framework to arrive at a more consistent picture of the equation of state of hadronic matter under extreme conditions [37] and the chiral

phase transition. Another interesting ramification [38] concerns the role of the medium-modified Δ spectral functions in the soft photon enhancement as recently observed at the SPS [39].

Acknowledgments

One of us (HvH) acknowledges support from the Alexander-von-Humboldt Foundation as a Feodor-Lynen Fellow.

References

- [1] Karsch F 2002 *Lect. Notes Phys.* **583** 209
- [2] Rapp R and Wambach J 2000 *Adv. Nucl. Phys.* **25** 1
- [3] Agakishiev G *et al.* (CERES/NA45) 1998 *Phys. Lett.* **B422** 405
- [4] Adamova D *et al.* (CERES/NA45) 2003 *Phys. Rev. Lett.* **91** 042301
- [5] Hjort E L *et al.* 1997 *Phys. Rev. Lett.* **79** 4345
- [6] Pelte D *et al.* (FOPI) 1997 *Z. Phys. A* **359** 55
- [7] Fachini P 2004 *J. Phys. G* **30** S735
- [8] Horikawa Y, Thies M and Lenz F 1980 *Nucl. Phys.* **A345** 386
- [9] Oset E and Salcedo L L 1987 *Nucl. Phys.* **A468** 631
- [10] Ericson T and Weise W 1988 *Pions and Nuclei* (Clarendon Press, Oxford)
- [11] Migdal A B, Saperstein E E, Troitsky M A *et al.* 1990 *Phys. Rept.* **192** 179
- [12] Xia L H, Siemens P J and Soyeur M 1994 *Nucl. Phys.* **A578** 493
- [13] Korpa C L and Lutz M F M 2004 *Nucl. Phys.* **A742** 305
- [14] Ko C M, Xia L H and Siemens P J 1989 *Phys. Lett.* **B231** 16
- [15] Korpa C L and Malfliet R 1995 *Phys. Rev. C* **52** 2756
- [16] van Hees H and Rapp R 2004 *Preprint* nucl-th/0407050
- [17] Cubero M 1990 Ph.D. thesis TH Darmstadt
- [18] Rapp R, Urban M, Buballa M *et al.* 1998 *Phys. Lett.* **B417** 1
- [19] Urban M, Buballa M, Rapp R *et al.* 2000 *Nucl. Phys.* **A673** 357
- [20] Nacher J C, Oset E, Vicente M J *et al.* 2001 *Nucl. Phys.* **A695** 295
- [21] Moniz E J 1981 *Nucl. Phys.* **A354** 535c
- [22] Weinhold W, Friman B and Nörenberg W 1998 *Phys. Lett.* **B433** 236
- [23] Hagiwara K *et al.* 2002 *Phys. Rev. D* **66** 01001
- [24] van Hees H and Knoll J 2002 *Phys. Rev. D* **65** 105005
- [25] Rapp R and Wambach J 1995 *Phys. Lett.* **B351** 50
- [26] Migdal A B 1978 *Rev. Mod. Phys.* **50** 107
- [27] Chanfray G and Schuck P 1993 *Nucl. Phys.* **A555** 329
- [28] Herrmann M, Friman B L and Nörenberg W 1993 *Nucl. Phys.* **A560** 411
- [29] Lepretre A *et al.* 1978 *Phys. Lett.* **B79** 43
- [30] Ahrens J *et al.* 1984 *Phys. Lett.* **B146** 303
- [31] Ahrens J 1985 *Nucl. Phys.* **A446** 229c
- [32] Frommhold T *et al.* 1992 *Phys. Lett.* **B295** 28
- [33] Frommhold T *et al.* 1994 *Z. Phys. A* **350** 249
- [34] Bianchi N *et al.* 1993 *Phys. Lett.* **B299** 219
- [35] Bianchi N *et al.* 1996 *Phys. Rev. C* **54** 1688
- [36] Rapp R 2002 *Phys. Rev. C* **66** 017901
- [37] Voskresensky D N 2004 *Preprint* hep-ph/0402020
- [38] Rapp R 2004 *Mod. Phys. Lett.* **A19** 1717
- [39] Aggarwal M M *et al.* (WA98) 2004 *Phys. Rev. Lett.* **93** 022301